Optical Transmittance Changes of Solid Preforms with Temperature II. Transparency of α-Al_2O_3 Ceramics after Sintering at 1250 °C

L. PACH, Ľ. BAČA, and J. MAJLING

Department of Ceramics, Glass, and Cement, Faculty of Chemical Technology, Slovak University of Technology, SK-812 37 Bratislava

Received 28 October 1999

Fe_2O_3 content controls the microstructure (porosity, pore size, grain size) and correspondingly an evolution of the light transmittance of gel monoliths based on boehmite. Porosity decreases with Fe_2O_3 content and it is completely eliminated in samples containing 6 mass % Fe_2O_3. Resulting polycrystalline material becomes thus transparent at temperatures as low as 1250 °C.

The transparent ceramics is often an ultimate goal in materials research and processing science. Transparency of the polycrystalline alumina, as well as of the other ceramics, is difficult to achieve due to light scattering by pores, grain boundaries, impurities, and other imperfections [1]. Standard procedures to prepare the transparent polycrystalline α-alumina ceramics rely on a doping of α-alumina powders, their isostatic pressing, and a two-step firing schedule [2]. The final heating takes place, however, at very high temperature (1800 °C).

In contrast, sol-gel, or colloidal routes may yield the transparent ceramics at low temperatures, the processing steps to control an evolution of the nano-size particle assemblies into adequate microstructures of the fired products, should, however, be quite deliberate. Sol-gel boehmite-derived alumina monoliths are usually transparent to about 1000 °C [3—7]. At higher temperatures, during concomitant sintering and transformation of defect alumina phases to stable α-Al_2O_3, the material becomes opaque [3].

Also in cases when the transparency is targeted property of the material, its *in situ* monitoring is not at all a common experimental procedure. The present *in situ* optical methods take mostly use of the reflected or reflectively scattered laser light [8—10]. Moreover, the usual methods of thermal analysis (DTA, TG) are wholly unrelated to the microstructure evolvement during the heating process.

In a former paper of this series the optical transmittance of thin hydroxyapatite pellets prepared by the high-pressure isostatic pressing has been investigated [11].

Presently, the solid preforms to be investigated are the colloidally consolidated thin boehmite planar monoliths, seeded by Fe_2O_3. Since the unseeded boehmite monoliths (thin gel fragments) had been notoriously transmitting from a rather high initial (green) transparency into full opaqueness at temperatures close to 1200 °C [12] the aim of this work was to extend the *in situ* transmittance measurements to boehmite gels seeded by Fe_2O_3. The sol seeding with α-Fe_2O_3 particles [13—15] or $Fe(NO_3)_3$ [16—18] has already been found an efficient way to lower the temperature of the γ- to α-alumina conversion. Presently, "seeds" have been introduced by means of the ferric nitrate solution.

EXPERIMENTAL

The boehmite gel monoliths used in this work were prepared from a commercial boehmite powder (Condea, specific surface area $\approx 250\ m^2\ g^{-1}$, particle size $\approx$ 10 nm) by the commonly used procedure [19]. A water-boehmite suspension ($\approx$ 10 mass %) and $Fe(NO_3)_3 \cdot 9H_2O$ (to yield α-Fe_2O_3 seeds) was peptized by mixing it with HNO_3 (pH of suspension about 2.5) at 55 °C. Fe_2O_3 seed contents are categorized in the following as 0F; 1F; 3F; 6F, corresponding to seed contents 0, 1, 3, and 6 mass % of Fe_2O_3 on α-Al_2O_3. The yellow nearly transparent boehmite sols were weighed in small plastic dishes (diameter $\approx$ 1.2 cm) in the quantity of 0.30 g. The sols were gelled from $\approx$ 10 min (6 mass % of Fe_2O_3) to 3 h (without seeding). The gels were allowed to dry at room temperature for 2 days. Afterwards, the dry gels monoliths were removed from dishes. The obtained gel discs with thickness $\approx 120\ \mu m$ were used in the subsequent experiments.

The on-line measurements of the optical transmittance were conducted in a computer-controlled vertical tube furnace with Pt-winding operating at temperatures up to 1350 °C, with built-in optical measuring system [11, 20, 21]. The Si-photodiode was used to evaluate the intensity of the transmitted light, recorded in 5 s intervals. A very soft light source of the light-emmitting diode ($\lambda \approx 570$ nm) has been found

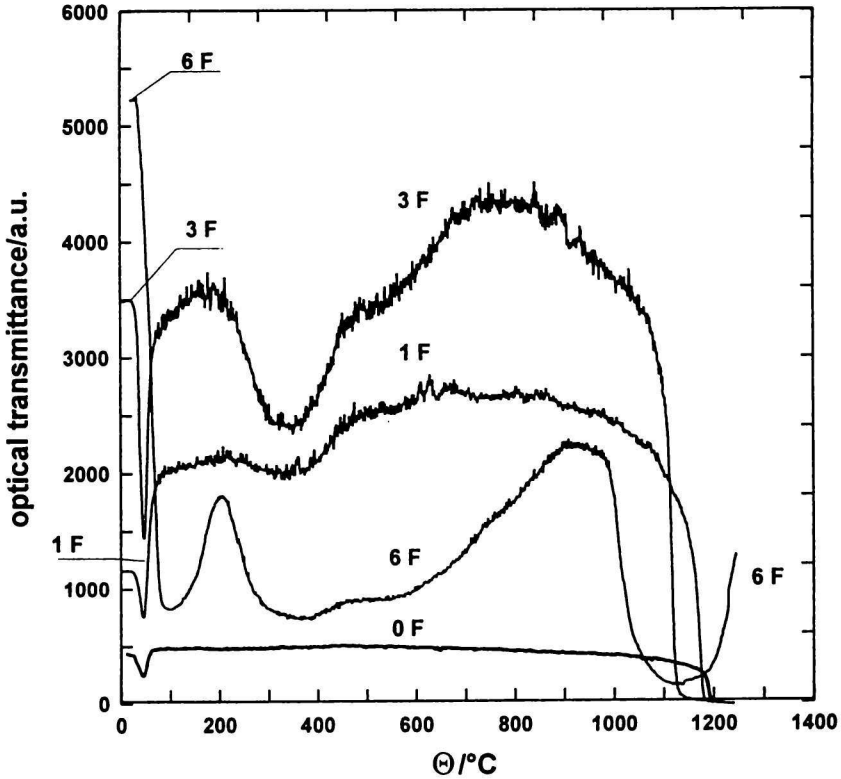

Fig. 1. Optical transmittance of boehmite gels *vs.* Fe_2O_3 seed content (0F – 0.0 mass %; 1F – 1.0 mass %; 3F – 3.0 mass %, and 6F – 6.0 mass % Fe_2O_3) and temperature; heating rate 10 °C min^{-1}, thickness of samples ≈ 100 μm.

suitable for performing experiments. At measurement the sample was supported on a Pt circular plate (1 mm thick) with an orifice (3 mm in diameter) to pass the light. The Pt/Rh thermocouple (S type), located in a close vicinity of the sample, was calibrated against melting point of K_2SO_4. The respective salt powder was in this case deposited in a thin layer on the saphire slide support, similarly as described in [22]. The heating rates adopted were 10 °C min^{-1}.

Thermal analyses (DTA, TG) of gels were carried out in air at a heating rate of 10 °C min^{-1} using a V1.9D TA instrument. The surface area and the pore size distribution in the nanometer scale were measured by N_2 adsorption and desorption isotherms (BET) using a Sorptomatic 1900. The microstructure of sintered samples was observed by SEM (Tesla BS 300).

RESULTS AND DISCUSSION

The colour of samples changes with iron content from the colourless character of the 0F sample (without iron) to the dark orange colour of the sample 6F.

The light transmittance of samples, as seen from Fig. 1, strongly depends on both, the temperature as well as the Fe_2O_3 seed content. For all samples there is a gradual increase of the room temperature transmittance with Fe_2O_3 content, as evident from start-points of the respective curves in Fig. 1. This suggests a positive effect of the $Fe(NO_3)_3$ additions on the colloidal self-assembling of the boehmite nano-particles during drying of the as cast gels. From this respect $Fe(NO_3)_3$ is expected to have a positive co-peptizing effect on boehmite particles.

A strong decrease in the optical transmittance of samples at 75 °C is caused by the exchange of capillary condensed water in the pores of sample monoliths with the air, in accord with DTA and TG recordings in Fig. 2. When the exchange is complete, the transmittances of samples 0F and 3F return to their initial values. The transmittance of 1F sample returns even to a higher value. The sample 6F behaves differently and a sudden decrease of its initial transmittance remains unexplained.

By comparison of curves in Fig. 1, it can be seen that the iron-free sample (0F) exhibits a low and steady-state transmittance until temperatures close to 1200 °C. Afterwards, the transmittance decreases to zero in a narrow temperature interval, similarly as observed in [12]. On account of the transparency changes one would expect an inferior particle packing of this sample in comparison to iron-containing samples. The set sample matrix is expected, in a sense, to prohibit the particle rearrangement in a heating course, having an effect of the unchanged sample's transmittance with temperature.

In contrast, samples doped by Fe_2O_3 show three local maxima in the transmittance. At the first maximum, at temperatures about 200 °C, the peak height

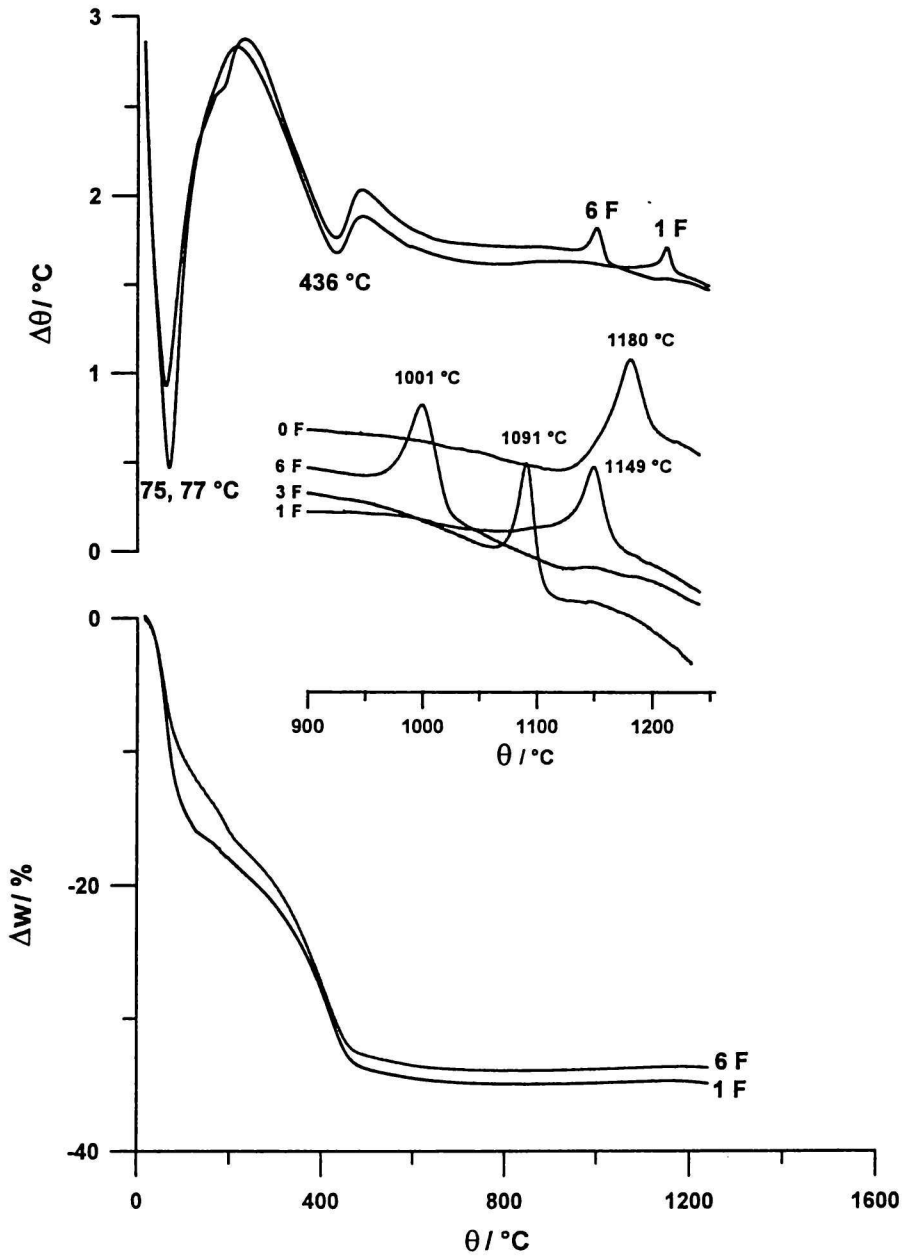

Fig. 2. DTA and TG of boehmite gels (samples 1F and 6F), crystallization of α-Al_2O_3 is shown for all samples in an insertion in figure.

increases with Fe_2O_3 content. This maximum has no corresponding thermal effects on DTA curves. The second maximum (at $\approx$ 500 °C) indicates the end of boehmite decomposition. The maximum rate of this decomposition is seen also well in endothermal effects on DTA curves at 436 °C and on the corresponding parts of TG records. The third maximum is very shallow for the sample 1F, becoming more pronounced for the sample 3F. The sample 6F behaves differently also at these temperatures. The respective transmittance maximum is much more resolved and significantly shifted to higher temperatures. This (third) maximum neither has the corresponding effects on DTA curves. The reason is a very small heat evolvement in underlying processes.

It can be well presumed that the transmittance increase means the microstructure refining, whereas a decrease its deterioration. So at temperatures corresponding to the ascending curve portions to the third maximum the microstructures are either changed very little (sample 1F, similarly to the sample 0F), or more profoundly (sample 3F). In a case of the sample 6F this positive ascend of the transmittance is, with respect to 3F sample, prolonged even to higher temperatures. The microstructure refinement, in this sense, would not include therefore processes like grain coarsening,

Table 1. Surface Area (s), Pore Specific Volume (v_p), Pore Radius (r_p), and Calculated Bulk Density (ρ) of Samples Heated up to 900 °C (without Soaking)

Sample	s	v_p	r_p	ρ
	$m^2\ g^{-1}$	$cm^3\ g^{-1}$	nm	$g\ cm^{-3}$
0F	170.0	0.375	3.7	1.60
1F	159.4	0.330	3.2	1.72
3F	155.7	0.303	3.5	1.81
6F	130.1	0.255	2.6	1.96

or pore growth, increasing the light scattering. They would mean, preferentially, the particle rearrangement resulting in their closer contacts. This hypothesis is supported by experiments discussed later.

From the third maximum, the light transmittances fall to zero values, with the exception of the 6F sample. The samples 0F—3F were fully opaque after their cooling to room temperature. They remained opaque also at their heating to 1600 °C.

The 6F sample behaved otherwise. It was interesting to notice that after an initial decrease of the transmittance, similar to the previous cases, the light intensity was not decreased to zero. The turn-point appeared at a temperature of 1160 °C, followed by an increase in the transmittance. From this portion of the curve one can literary see rates and temperature ranges of the microstructure deterioration and the further refining process, as pointed out previously. The transition between negative and positive microstructure evolvement processes actually takes place, in this case, at a temperature of ≈1000 °C, as also seen in [23]. This sample remained well transparent on its cooling to room temperature and also at its subsequent heating to 1600 °C.

Since the gel monoliths were losing their transparency at temperatures above 900 °C, two sets of new samples were prepared with thermal treatment similar to that one at the optical transmittance measurements. The gel monoliths of the first set were all heated at a rate of 10 °C min^{-1} to 900 °C, with followed cooling to room temperature. The gel monoliths of the second set were individually heated to temperatures (t^*) at which, according to the former OT experiments, the corresponding transmittances were decreased to their half values (Fig. 1). Both sets of samples were examined for properties listed in Table 1. In DTA analyses it was found out that the selected t^* temperatures were very close to exothermal effects

Table 2. Surface Area (s), Pore Specific Volume (v_p), Pore Radius (r_p), and Calculated Bulk Density (ρ) of Samples at Temperature t^* (without Soaking). Temperatures t^* are near to DTA Peak of α-Al_2O_3 Crystallization (t_{max})

Sample	t^*	t_{max}	s	v_p	r_p	ρ
	°C	°C	$m^2\ g^{-1}$	$cm^3\ g^{-1}$	nm	$g\ cm^{-3}$
0F	1190	1180	20.0	0.120	28.3	2.73
1F	1160	1149	15.8	0.083	23.5	3.04
3F	1100	1091	16.4	0.066	17.5	3.16
6F	1000	1001	31.1	0.191	6.5	2.27

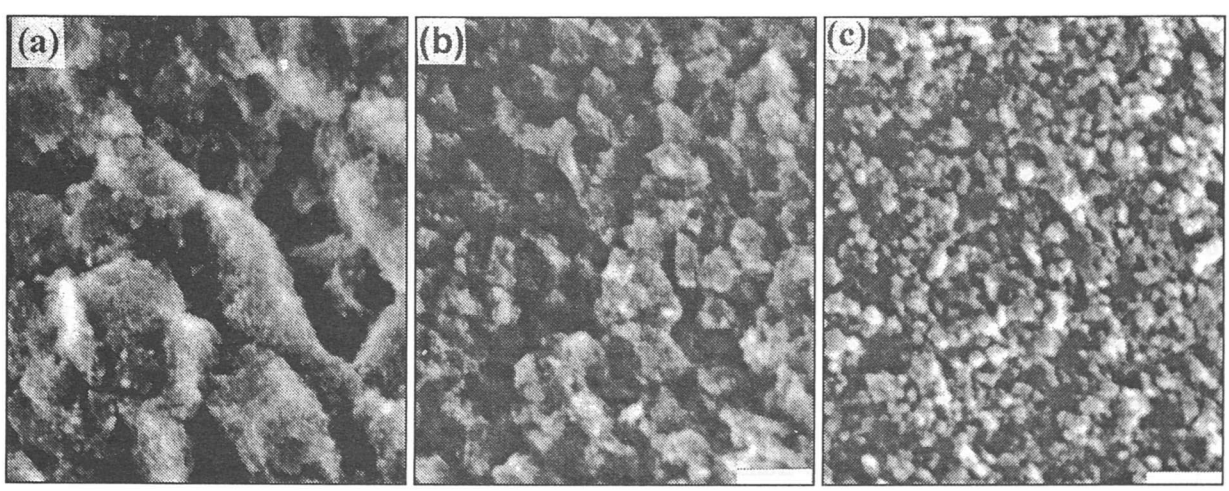

Fig. 3. SEM micrographs (bar = 2.5 μm) of fracture surface of samples 1F (*a*), 3F (*b*), 6F (*c*) heated to 1250 °C (heating rate 10 °C min^{-1}, F means $w(Fe_2O_3)/\%$ in Al_2O_3).

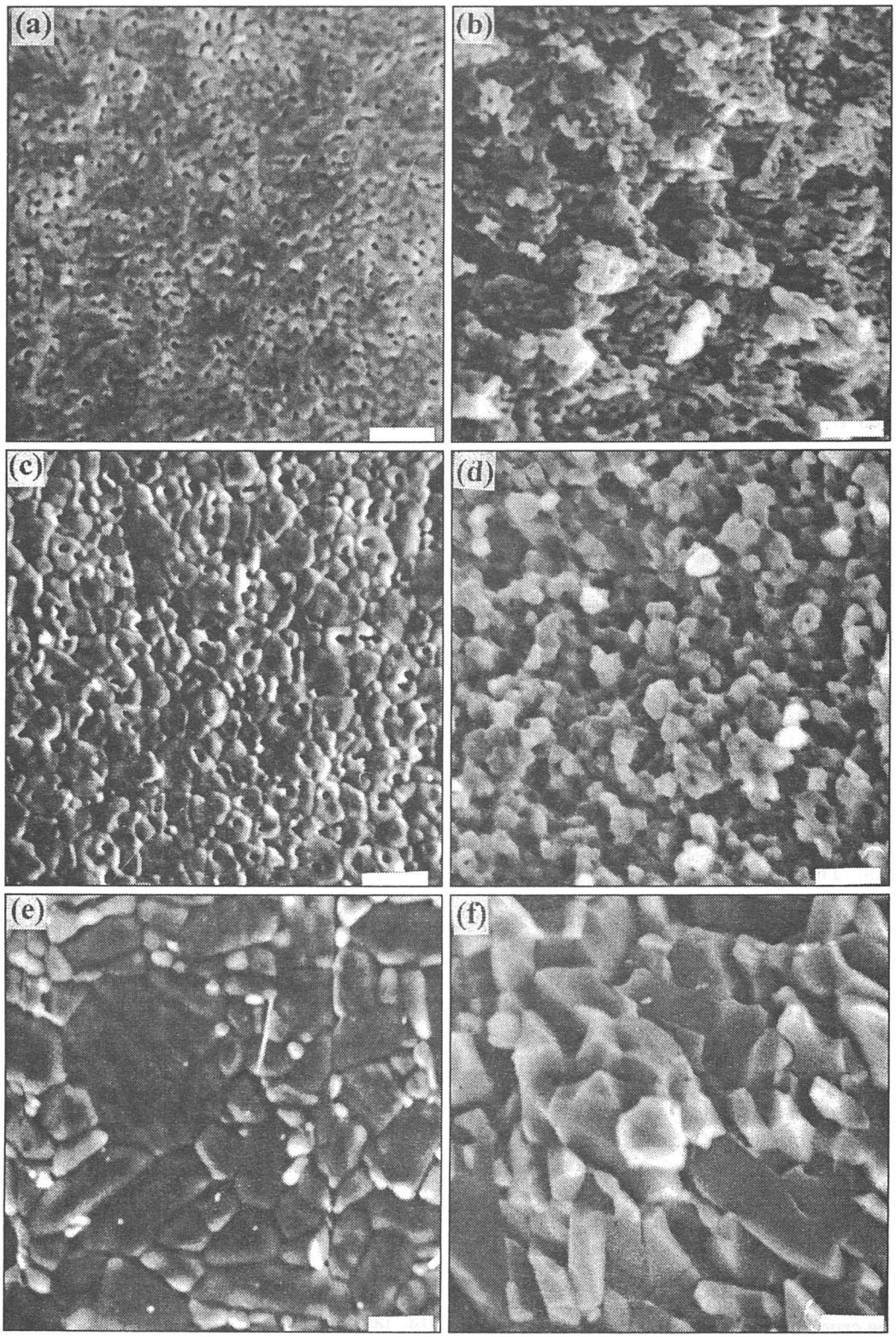

Fig. 4. SEM micrographs (bar = 2.5 μm) of samples heated for 1 h at 1350 °C (heating rate 10 °C min^{-1}): 1F (*a*, *b*), 3F (*c*, *d*), 6F (*e*, *f*), natural surfaces (*a*), (*c*), (*e*), fracture surfaces (*b*), (*d*), (*f*) (F means $w(Fe_2O_3)/\%$ in Al_2O_3).

of the α-Al_2O_3 crystallization (an insertion in Fig. 2). This is an independent proof that a decrease of the transmittance is related to α-alumina crystallization.

The microstructure changes above 900 °C are most decisive ones since they lead either to the final samples' transparency, or full opacity. The surface area, pore volume, and pore size of all samples (Table 1) do not differ significantly at 900 °C. The samples are

transparent, since the nanometer-size pores do not scatter the light. At t^* temperatures (Table 2), the significant decrease in the surface area and the pore volume is contrasting an increase in size of pores. These changes are caused by sintering and the concomitant crystallization of α-Al_2O_3. They are significantly influenced by the content of Fe_2O_3. Annealing of 0F, 1F, and 3F samples at 1350 °C (1 h) leads to a coalescence of pores to the micron size (Fig. 4), whereas the pores of the 6F sample are completely eliminated at these temperatures.

The microstructure of sintered samples was observed by SEM, after the transmittance measurements (reaching $\approx$ 1250 °C and cooling down the samples from this temperature) and after a separate heat treatment at 1350 °C for 1 h. The former samples show differing microstructures on fracture surfaces (Fig. 3), but the same on free surfaces. Samples 0F and 1F behaved identically, therefore only SEM micrograph of the sample 1F is presented. The size of the microstructure elements in Fig. 3 decreases in the sequence 1F $\rightarrow$ 3F $\rightarrow$ 6F (5—0.5 μm). Pores are too small for observation at the magnification used. More revealing are the SEM pictures after 1 h heating at 1350 °C (Fig. 4). Sample 1F contains a homogeneous porous structure (Fig. 4*a*, *b*) known as the vermicular structure [15], while sample 3F (Fig. 4*c*, *d*) contains 1 or 2 pores usually in the middle of the crystals. Sample 6F (Fig. 4*e*, *f*) is pore-free with a size of crystals in the range of 2—7 μm.

It is well known that the crystallization of α-Al_2O_3 in boehmite-derived gels needs homogeneous nucleation [15, 19]. This nucleation is quite difficult and is limited by the number of nucleation sites. The latter are the colloidal particles with the highest (12) coordination [19] as demonstrated by cold isostatic pressing of gels (1.5 GPa) [24]. Crystallization of α-Al_2O_3 is spread radially from the nucleus until the crystallization zones collide with zones of neighbouring nuclei. Such processes result in a porous vermicular [15, 19, 25] microstructure of the material (Fig. 3*a*).

The described mechanism of α-alumina crystallization is more and more suppressed by an increasing content of Fe_2O_3. Sample 3F contains only one or two pores per grain (Fig. 4*c*, *d*) while sample 6F is completely without visible (SEM) pores (Fig. 4*e*, *f*) as a consequence of the heterogeneous nucleation effect of Fe_2O_3.

Because the transparency strongly depends on porosity, the crucial requirement for transparency was the removal of pores at sufficient content of Fe_2O_3 (sample 6F). At lower contents of Fe_2O_3, pores do not vanish, but oppositely, they grow to the micron size causing the scattering of light.

CONCLUSION

Processes taking place during heating of boehmite gel monoliths such as drying, phase transformation, or pore growth are reflected by the on-line measurement of the light transmittance. It was shown here that all these processes are controlled by Fe_2O_3 content.

The temperature of α-Al_2O_3 crystallization, the porosity and the pore size of sintered bodies decrease with Fe_2O_3 content, producing the transparency of respective ceramics at 6 mass % of Fe_2O_3 content, and a temperature of 1250 °C. Further increase of transparency is associated with the increase in size of the grains of pore-free bodies.

It was further ascertained that optical transmittance measurements are indicative also of microstructure transforms, connected with very minute thermal effects, not identified by DTA. Moreover, the optical transmittance is suggested to be a convenient measure for the efficiency of the colloidal particle packing at wet forming procedures.

Acknowledgements. This research was supported by the U.S.-Slovak Science and Technology Joint Fund Project No. 011-95 and by the Slovak VEGA Grant No. 1/6116/99.

REFERENCES

1. Kingery, W. D., Bowen, H. K., and Uhlmann, D. R., *Introduction to Ceramics,* Second Edition. P. 674. Wiley and Sons, New York, 1976.
2. Lee, D. W. and Kingery, W. D., *J. Am. Ceram. Soc. 43*, 594 (1960).
3. Grimm, N., Scott, G. E., and Sibold, J. D., *Am. Ceram. Soc. Bull. 50*, 962 (1971).
4. McClelland, J. D. and Zehms, E. H., *J. Am. Ceram. Soc. 46*, 77 (1963).
5. Kurokawa, Y., Shirakawa, T., Saito, S., and Yui, N., *J. Mater. Sci. Lett. 5*, 1070 (1986).
6. Sasaki, H., Kobayashi, Y., Muto, S., and Kurokawa, Y., *J. Am. Ceram. Soc. 73*, 453 (1990).
7. Gallas, M. R., Hockey, B., Pechenik, A., and Piermarini, G. J., *J. Am. Ceram. Soc. 77*, 2107 (1994).
8. Raether, F., Hofmann, R., Müller, G., and Sölter, H. J., *J. Therm. Anal. Calorim. 53*, 717 (1998).
9. Simpson, T. V. Q., Wen, N. Yu., and Clarke, D. R., *J. Am. Ceram. Soc. 81*, 61 (1998).
10. Shur, V. Ya., Negashev, S. A., Subbotin, A. L., Pelegov, D. V., Borisova, E. A., Blankova, E. B., and Trolier-McKinstry, S. E., *Phys. Solid State 41*, 274 (1999).
11. Ďurovčíková, R., Kremničan, V., Kovalík, Š., Svetík, Š., Krištín, J., Marquis, P. M., and Majling, J., *Chem. Pap. 53*, 16 (1999).
12. Pach, L., Majling, J., and Komarneni, S., *J. Sol-Gel Sci. Technol.*, submitted for publication.
13. Levin, I. and Brandon, D., *J. Am. Ceram. Soc. 81*, 1995 (1998).
14. McArdle, J. L. and Messing, G. L., *Adv. Ceram. Mater. 3*, 387 (1988).
15. McArdle, J. L. and Messing, G. L., *J. Am. Ceram. Soc. 76*, 214 (1993).
16. Polli, A. D., Lange, F. F., Levi, C. G., and Mayer, J., *J. Am. Ceram. Soc. 79*, 1745 (1996).
17. Tartaj, J. and Messing, G. L., *J. Eur. Ceram. Soc. 17*, 719 (1997).

18. Oberbach, Th., Günther, C., Werner, G., and Tomandl, G., Feiberg: cfi/*Ber. DKG 74*, No. 11/12 (1997).
19. Pach, L., Roy, R., and Komarneni, S., *J. Mater. Res. 5*, 278 (1990).
20. Majling, J., Svetík, Š., Annus, J., Krištín, J., and Marquis, P. M., *Chem. Pap. 51*, 268 (1997).
21. Majling, J., Kremničan, V., Ďurovčíková, R., and Svetík, Š., *J. Therm. Anal. Calorim. 57*, 587 (1999).
22. Majling, J., Svetík, Š., Kremničan, V., and Chocholoušek, J., *Ceramics - Silikáty 43*, 71 (1999).
23. Majling, J., Svetík, Š., and Pach, L., *Key Engineering Materials*, Vols. *175—176*, p. 91 (2000).
24. Pach, L., Kovalík, Š., Majling, J., and Kozánková, J., *J. Eur. Ceram. Soc. 12*, 249 (1993).
25. Dynys, F. W. and Halloran, J. W., *J. Am. Ceram. Soc. 65*, 442 (1982).